ECCM-2001

European Conference on
Computational Mechanics

June 26-29, 2001
Cracow, Poland

A P-ADAPTIVE SCHEME FOR OVERCOMING VOLUMETRIC LOCKING DURING ISOCHORIC PLASTIC DEFORMATION

G. N. Wells and L. J. Sluys

Koiter Institute Delft
Delft University of Technology, Delft, The Netherlands
e–mail: g.wells@citg.tudelft.nl

Key words: volumetric locking, plasticity, adaptivity, partition of unity.

Abstract. *A p-adaptive scheme is developed in order to overcome volumetric locking in low order finite elements. A special adaptive scheme is used which is based on the partition of unity concept. This allows higher order polynomial terms to be added locally to the underlying finite element interpolations basis through the addition of extra degrees of freedom at existing nodes. During the adaptive process, no new nodes are added to the mesh. Volumetric locking is overcome by introducing higher order polynomial terms in regions where plastic flow occurs. The model is able to overcome volumetric locking for plane strain, axisymmetric and three-dimensional problems.*

---

1 Introduction

Volumetric locking in low-order finite elements during plastic flow is an enduring problem in computational plasticity. When using low-order finite elements, volumetric locking leads to an over-prediction of the collapse load or leads to a hardening-like response making it impossible to predict a collapse load.

This poor response in light of the popularity of low-order finite elements is unfortunate, and has stimulated much research into improving the performance of low-order finite elements during isochoric and dilatant/contractive plastic deformation. The most simple approach for overcoming volumetric locking under plane strain conditions when using linear triangles is the use of crossed triangle patches [1]. This simple and popular approach is effective for many cases, although it breaks down under axisymmetric conditions and can prove difficult when meshing on complex geometries. Another approach is to interpolate the hydrostatic pressure and displacements separately, leading to extra nodal or internal degrees of freedom. However, it is difficulty to construct such elements using linear triangles that satisfy the necessary stability conditions [2]. For four-noded quadrilaterals elements, there exist several solutions for overcoming volumetric locking. Most methods involve modifications of the strain field. One method is the B-bar approach [3], however this method fails for dilatant or contractive plastic flow [4]. So-called Enhanced Assumed Strain (EAS) methods [5] have been used to effectively overcome volumetric locking in quadrilateral elements, although the method fails for elements with triangular geometry [6].

None of the above mentioned methods are effective for overcoming volumetric locking in elements based on triangular geometry for plane strain, axisymmetric and three-dimensional cases. This is despite elements based on triangular geometry being popular in use and highly suited for meshing irregular geometries. The only robust solution for overcoming volumetric locking in all cases in the use of higher order finite elements [7]. This concept is followed here, with a new adaptive scheme proposed for overcoming volumetric locking during plastic flow using low-order elements based on triangular geometry. The partition of unity concept [8–10] is used to develop a p-adaptive scheme which allows the displacement interpolation to be enriched locally without the addition of extra nodes to the mesh. The amplitudes of higher order polynomial terms added to the interpolation are represented by extra degrees of freedom at existing nodes.

The proposed adaptive method is illustrated through numerical examples. Plane strain, axisymmetric and three-dimensional examples are analysed using a perfectly plastic Von Mises model.

2 Adaptive formulation

It has been shown that a field u over a volume Ω can be interpolated by [8–10]:

$$u(\mathbf{x}) = \sum_{i=1}^{n_{\mathrm{n}}} \varphi_i(\mathbf{x}) \left(a_i + \sum_{j=1}^{n_{\mathrm{basis}}} \gamma_j(\mathbf{x}) b_{ij} \right) \tag{1}$$

where $\boldsymbol{\varphi}$ is a collection of functions forming a partition of unity, $\mathbf{x} \in \Omega$ is the spatial position, n_{n} is the total number of discrete nodal points, a_i is a discrete value associated with the discrete point (nodal point) i, γ_j contains n_{basis} basis functions and b_{ij} contains n_{basis} discrete values associated with each nodal point i. A collection of functions $\boldsymbol{\varphi}$ forms a partition of unity if:

$$\sum_{i=1}^{n_{\text{n}}} \varphi_i(\mathbf{x}) = 1. \tag{2}$$

By using finite element shape functions as partitions of unity, it is possible to use equation (1) to facilitate a form of p-adaptivity. The nodal values a_i can be considered the 'regular' nodal degrees of freedom and the nodal values b_{ij} can be considered as 'enhancements'. By using finite element shape functions as partition of unity functions and by adding 'enhanced' degrees of freedom to a node, the support of that node is enhanced. Crucially, enhancements can be introduced node-per-node, so only nodes requiring enhancement have extra degrees of freedom. The key difference with hierarchical methods [11] is that extra degrees of freedom are located at existing nodes, rather than at mid-side points or within an element.

In finite element notation, the displacement field with enhancements is expressed as:

$$\mathbf{u}(\mathbf{x}) = \mathbf{N}(\mathbf{x})\mathbf{a} + \mathbf{N}(\mathbf{x})\mathbf{N}_\gamma(\mathbf{x})\mathbf{b} \tag{3}$$

where $\mathbf{u}$ is a vector containing the displacement components, $\mathbf{N}$ contains the usual matrix containing the element shape functions N_i, $\mathbf{N}_\gamma$ is a matrix containing enhanced basis terms $\boldsymbol{\gamma}$ and the vector $\mathbf{b}$ contains the enhanced degrees of freedom. The strain field is expressed:

$$\boldsymbol{\varepsilon}(\mathbf{x}) = \mathbf{B}(\mathbf{x})\mathbf{a} + \mathbf{B}_\gamma(\mathbf{x})\mathbf{b} \tag{4}$$

where $\mathbf{B}$ is of the usual form containing spatial derivatives of the shape functions and $\mathbf{B}_\gamma$ contains spatial derivatives of $\mathbf{N}\mathbf{N}_\gamma$.

For a single node i the matrix containing the enhanced basis terms is of the form:

$$\mathbf{N}^i_\gamma = \begin{bmatrix} \gamma_1 & \gamma_2 & \cdots & \gamma_{n_{\text{basis}}} & 0 & 0 & \cdots & 0 & 0 & 0 & \cdots & 0 \\ 0 & 0 & \cdots & 0 & \gamma_1 & \gamma_2 & \cdots & \gamma_{n_{\text{basis}}} & 0 & 0 & \cdots & 0 \\ 0 & 0 & \cdots & 0 & 0 & 0 & \cdots & 0 & \gamma_1 & \gamma_2 & \cdots & \gamma_{n_{\text{basis}}} \end{bmatrix}. \tag{5}$$

The matrix $\mathbf{B}_\gamma$ for a node i is of the form:

$$\mathbf{B}^i_\gamma = \begin{bmatrix} \frac{\partial(N_i\gamma_1)}{\partial x} & \cdots & \frac{\partial(N_i\gamma_{n_{\text{basis}}})}{\partial x} & 0 & \cdots & 0 & 0 & \cdots & 0 \\ 0 & \cdots & 0 & \frac{\partial(N_i\gamma_1)}{\partial y} & \cdots & \frac{\partial(N_i\gamma_{n_{\text{basis}}})}{\partial y} & 0 & \cdots & 0 \\ 0 & \cdots & 0 & 0 & \cdots & 0 & \frac{\partial(N_i\gamma_1)}{\partial z} & \cdots & \frac{\partial(N_i\gamma_{n_{\text{basis}}})}{\partial z} \\ \frac{\partial(N_i\gamma_1)}{\partial y} & \cdots & \frac{\partial(N_i\gamma_{n_{\text{basis}}})}{\partial y} & \frac{\partial(N_i\gamma_1)}{\partial x} & \cdots & \frac{\partial(N_i\gamma_{n_{\text{basis}}})}{\partial x} & 0 & \cdots & 0 \\ 0 & \cdots & 0 & \frac{\partial(N_i\gamma_1)}{\partial z} & \cdots & \frac{\partial(N_i\gamma_{n_{\text{basis}}})}{\partial z} & \frac{\partial(N_i\gamma_1)}{\partial x} & \cdots & \frac{\partial(N_i\gamma_{n_{\text{basis}}})}{\partial x} \\ \frac{\partial(N_i\gamma_1)}{\partial z} & \cdots & \frac{\partial(N_i\gamma_{n_{\text{basis}}})}{\partial z} & 0 & \cdots & 0 & \frac{\partial(N_i\gamma_1)}{\partial y} & \cdots & \frac{\partial(N_i\gamma_{n_{\text{basis}}})}{\partial y} \end{bmatrix}. \tag{6}$$

The format of the enhancement makes it straightforward to implement in standard finite element codes. It is stressed that the adaptive procedure does not require the introduction of any additional nodal points or special constraints, as is needed for conventional p-adaptive procedures.

3 Local polynomial enrichment to overcome volumetric locking

To enhance linear triangular elements, whose shape functions contain polynomial terms up to x and y, quadratic enhancement can be achieved using the enhanced basis:

$$\boldsymbol{\gamma}^{p=2}_{n_{\text{spat}}=2} = \left\{ \left(x-x_i\right)^2, \ \left(x-x_i\right)\left(y-y_i\right), \ \left(y-y_i\right)^2 \right\} \tag{7}$$

where x and y are spatial coordinates, x_i and y_i are the spatial coordinates of the node being enhanced and n_{spat} is the spatial dimension. This basis is of the form used by [12] to enhance linear triangles. It was shown by [12] that linear triangles enhanced by the basis in equation (7) pass the patch test in arrangements of more than one element. The equivalent quadratic enhanced basis for four-noded tetrahedral elements is of the form:

$$\begin{aligned}\boldsymbol{\gamma}^{p=2}_{n_{\text{spat}}=3} = \Big\{ &\left(x-x_i\right)^2, \ \left(x-x_i\right)\left(y-y_i\right), \ \left(x-x_i\right)\left(z-z_i\right), \ \left(y-y_i\right)^2, \\ &\left(y-y_i\right)\left(z-z_i\right), \ \left(z-z_i\right)^2 \Big\}. \end{aligned} \tag{8}$$

Note that the polynomial enhancement is centred at a node. This avoids difficulties with numerical conditioning if a node is located far from the origin.

An attractive feature of this approach is that it involves only the linear shape functions. There is no need to develop higher order shape functions to achieve a higher order of interpolation, nor are mid-side nodes required. It is possible to shown that the proposed enhancement leads to a formulation capable to reproducing complete quadratic polynomials. The reader is referred to [12] and [13] for details.

To overcome locking, quadratic enhancements are added locally to nodes in regions where plastic flow is occurring. More specifically, when plastic flow is detected at an integration point, all nodes whose support contains the integration points are enhanced. In implementation, a calculation is performed using linear base elements, and when plastic flow is detected, nodes are enhanced. To simplify the implementation, nodes at which essential boundary conditions are imposed are not enhanced. This simplifies greatly the imposition of essential boundary conditions.

4 Numerical examples

To test the adaptive scheme for overcoming volumetric locking, a series of punch tests are performed under plane strain and axisymmetric conditions and in three-dimensions. The simulations are performed using a perfectly plastic Von Mises model. The material parameters are taken as: Young's modulus $E = 1.0$ MPa, Poisson's ratio $\nu = 0.49$ and yield strength $\bar{\sigma} = 0.01$ MPa. For two-dimensional examples, linear triangles are used as the underlying element for enhancement and in three-dimensions, linear tetrahedra are used as the underlying element.

The discussion in this section focuses on overcoming volumetric locking. A discussion over the efficiency and the number of extra degrees of freedom required can be found in [13].

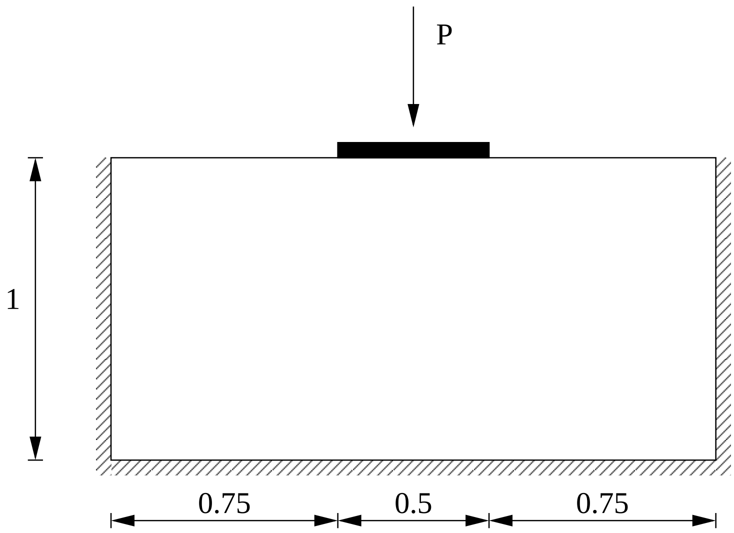

Figure 1: Plane strain punch test configuration. All dimensions in millimetres.

4.1 Plane strain

To test the model under plane strain conditions, Prandtl's punch test is analysed. An infinitely stiff plate is pushed into a semi-infinite halfspace. The test is illustrated in figure 1. The test is analysed for four different cases. The first case involves standard linear triangular elements in a diagonal arrangement. The mesh used is shown in figure 2a. The second case involves a mesh of crossed linear triangular elements, a configuration which is known to exhibit a locking-free response under plane strain conditions. The crossed triangle mesh is shown in figure 2b. The third case uses the mesh shown in figure 2a, with quadratic elements. The adaptive model is the fourth case, using the diagonal mesh in figure 2a.

The load-displacement responses for the four cases are shown in figure 3. Standard linear triangles in the diagonal mesh configuration clearly exhibit a locking response, with no peak load approached. As expected, the crossed linear triangle arrangement and the quadratic triangles do not lock, reaching a flat plateau in the load–displacement responses. The adaptive model using the diagonal linear triangles as the underlying element also does not lock, with a response that is indistinguishable from the crossed triangles arrangement. The adaptive mesh shows an overly stiff response in the elastic stage since the adaptive scheme does not overcome locking of the elastic response. For typical elasto-plastic calculations where elastic strains are small compared to plastic strains, this is of little consequence and is only an issue when the elastic response is nearly incompressible.

4.2 Axisymmetric

A similar test to the plane strain example is analysed for the axisymmetric case. An infinitely stiff circular plate (radius = 0.25mm) is pushed into the centre of a cylinder of radius = 1mm and depth = 1mm. The sides and lower boundary of the cylinder are fully restrained. Again, four different cases are tested: diagonal linear triangles (figure 4a); crossed linear triangles (figure 4b);

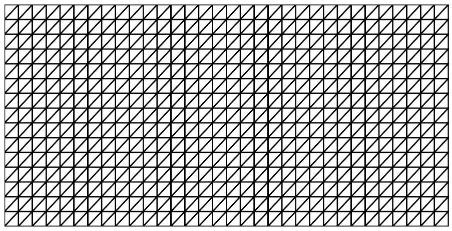

(a)

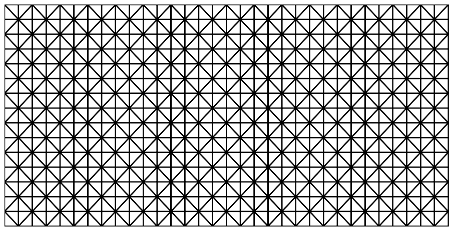

(b)

Figure 2: Discretisations for plane strain analyses with (a) diagonal and (b) crossed triangles. Both meshes are constructed with 960 elements.

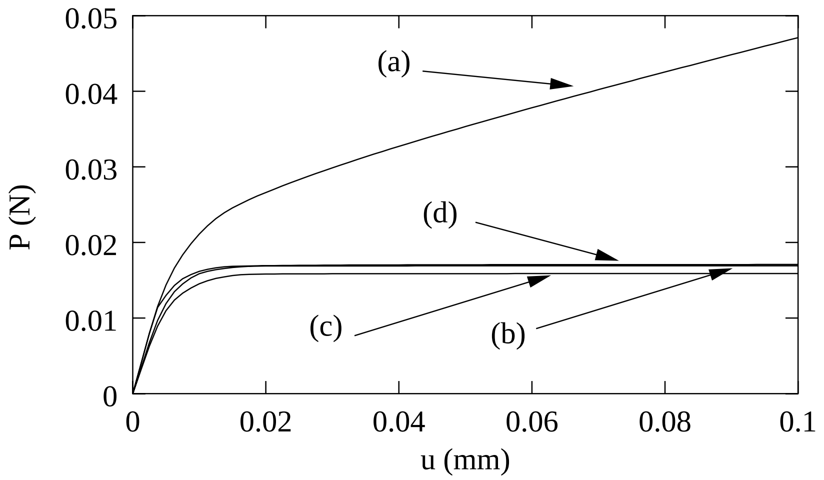

Figure 3: Load–displacement response for the plane strain punch test with (a) diagonal linear triangles, (b) crossed linear triangles, (c) diagonal quadratic triangles and (d) diagonal linear triangles with enhancement.

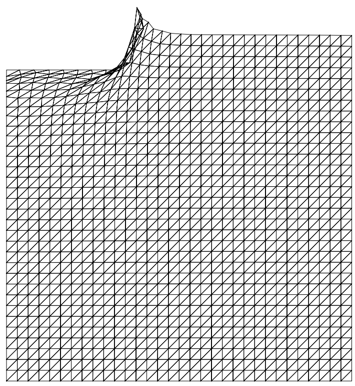

(a)

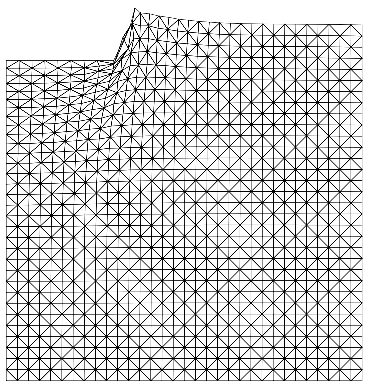

(b)

Figure 4: Discretisations (in deformed configuration) for axisymmetric analyses with (a) diagonal (with enhancement) and (b) crossed triangles. Both meshes are constructed with 2048 elements.

diagonal quadratic triangles (figure 4a); and enhanced diagonal linear triangles (figure 4a). The two different meshes used are shown in figure 4. The meshes are shown in the deformed configuration.

The load–displacement responses for the four cases are shown in figure 5. Again, as expected, the diagonal linear triangles exhibit a severe locking response. The crossed triangles arrangement also exhibits a locking response, although less severe than the diagonal arrangement. The enhanced model however does not exhibit locking, and predicts a peak load very close to the response predicted by the mesh constructed with quadratic triangular elements.

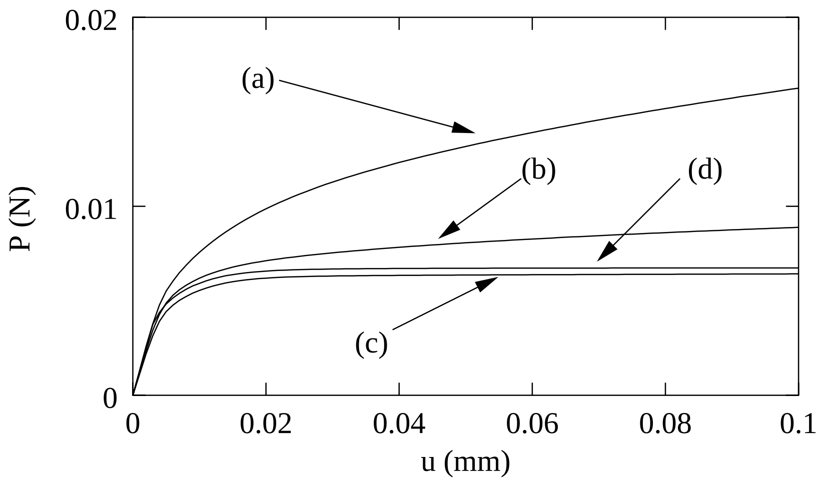

Figure 5: Load–displacement response for the axisymmetric punch test with (a) diagonal linear triangles, (b) crossed linear triangles, (c) diagonal quadratic triangles and (d) diagonal linear triangles with enhancement.

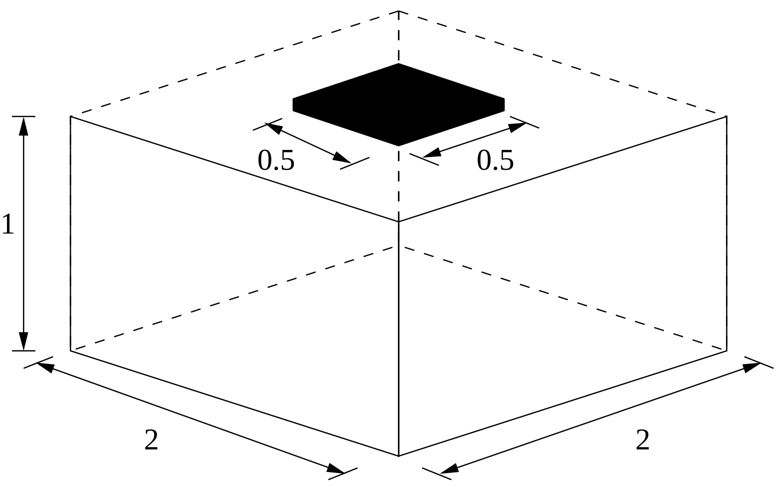

Figure 6: Three-dimensional punch test. The bottom and side surfaces of the prism are fully restrained and the infinitely stiff plate is located in the centre of the top surface. All dimensions in millimetres.

4.3 Three-dimensional

The three-dimensional punch test is shown in figure 6. The plate in assumed to be infinitely stiff and is pushed into the box. The sides and bottom of the box are fully restrained. The three-dimensional punch test is performed for two cases, the first with standard linear tetrahedra and the second with enhanced linear tetrahedra. The mesh used for the analysis, in a deformed configuration, is shown in figure 7. Using symmetry, only one quarter of the box is modelled.

The load–displacement responses for the three-dimensional punch test are shown in figure 8. The standard linear tetrahedra exhibit a severe locking response, while the enhanced mesh is able to predict a peak load and avoid volumetric locking.

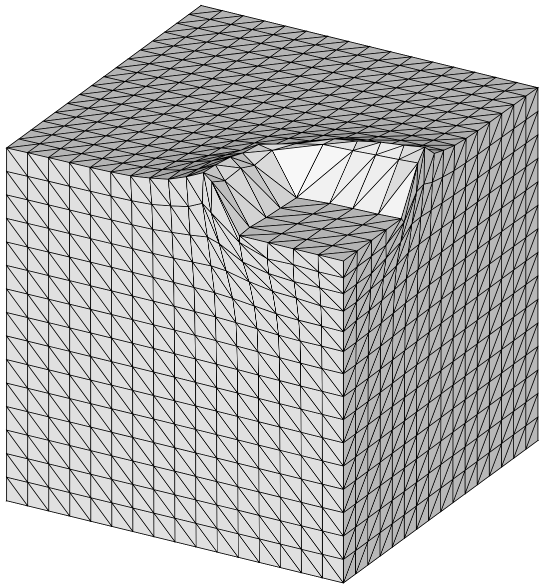

Figure 7: Deformed three-dimensional mesh for the punch simulation. Using symmetry, only one quarter of the block is modelled.

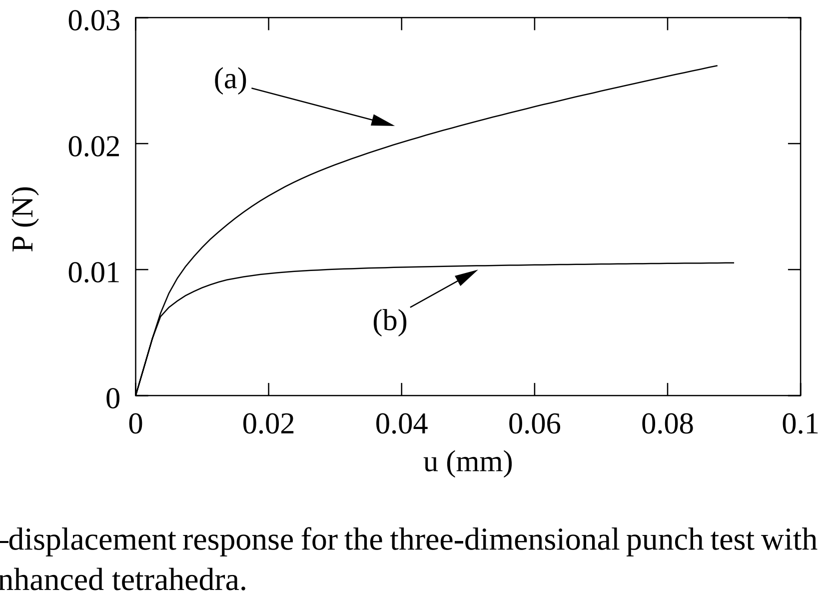

Figure 8: Load–displacement response for the three-dimensional punch test with (a) linear tetrahedra and (b) enhanced tetrahedra.

5 Conclusions

A p-adaptive scheme has been developed which allows volumetric locking to be robustly and efficiently overcome during localised plastic flow. Using the partition of unity concept, the finite element interpolation order is increased in regions where plastic flow is occurring. This is done through the addition of extra degrees of freedom at existing nodes, rather than adding extra nodal points. The method has been shown to be effective for plane strain, axisymmetric and three dimensional cases using linear underlying finite elements. The method is potentially very efficient since degrees of freedom are added only to regions where plastic flow is occurring. The method is also simple in implementation since it involves low order shape functions and mesh generation is simplified since only apex nodes are required.

References

[1] J. C. Nagtegaal, D. M. Parks, and J. R. Rice. On numerically accurate finite elements solutions in the fully plastic range. *Computer Methods in Applied Mechanics and Engineering*, **4**, 153–178, (1974).

[2] O. C. Zienkiewicz and R. L. Taylor. *The Finite Element Method. Volume 1: Basic Formulations and Linear Problems*. McGraw-Hill Book Company, fourth edition, (1994).

[3] T. J. R. Hughes. Generalization of selective integration procedures to anisotropic and nonlinear media. *International Journal for Numerical Methods in Engineering*, **15**(2), 1413–1418, (1980).

[4] R. De Borst and A. E. Groen. Some observations on element performance in isochoric and dilatant plastic flow. *International Journal for Numerical Methods in Engineering*, **38**(17), 2887–2906, (1995).

[5] J. C. Simo and M. S. Rifai. A class of mixed assumed strain methods and the method of incompatible modes. *International Journal for Numerical Methods in Engineering*, **29**(8), 1595–1638, (1990).

[6] B. D. Reddy and J. C. Simo. Stability and convergence of a class of enhanced strain methods. *SIAM Journal on Numerical Analysis*, **32**(6), 1705–1728, (1995).

[7] S. W. Sloan and M. F. Randolph. Numerical prediction of collapse loads using finite element methods. *International Journal for Numerical and Analytical Methods in Geomechanics*, **6**, 47–76, (1982).

[8] J. M. Melenk and I. Babuška. The partition of unity finite element method: Basic theory and applications. *Computer Methods in Applied Mechanics and Engineering*, **139**(1–4), 289–314, (1996).

[9] I. Babuška and J. M. Melenk. The Partition of Unity Method. *International Journal for Numerical Methods in Engineering*, **40**(4), 727–758, (1997).

[10] C. A. Duarte and J. T. Oden. H-p clouds – an h-p meshless method. *Numerical Methods for Partial Differential Equations*, **12**(6), 673–705, (1996).

[11] O. C. Zienkiewicz, J. P. De S. R. Gago, and D. W. Kelly. The hierarchical concept in finite element analysis. *Computers and Structures*, **16**(1–4), 53–65, (1983).

[12] R. L. Taylor, O. C. Zienkiewicz, and E. Oñate. A hierarchical finite element method based on the partition of unity. *Computer Methods in Applied Mechanics and Engineering*, **152**(1–2), 73–84, (1998).

[13] G. N. Wells and L. J. Sluys. A p-adaptive scheme for overcoming volumetric locking during plastic flow. *Computer Methods in Applied Mechanics and Engineering*, , (2001). (submitted).